





(i.e. corner reflectors) changes are more pronounced and more suitable for urban damage assessment as used in this study

Nevertheless, the presence of false assignments, random objects (moving object such as cars) and also feature changes observed in the nature are unavoidable. Considering “before” and “after” images and summarizing the difference values of the calibrated Xp index for individual buildings, a preliminary damage map is generated. This map is created considering the following main steps.

**Ancillary Data–Parcel Information:** The scope of present research is to compile high resolution city data with parcel level of details including the city topography and building height information and other attributed data. The parcel maps and building height information were mainly extracted from 1:2000 scale digital maps provided by National Cartographic Center (NCC) of Iran. These maps were created by processing aerial stereo-photographs. The extracted city parcel information have been processed and compiled from different sets of data that required both spatial adjustments and temporal change considerations. The parcel layer was complemented and updated using VHR (very high resolution) optical satellite image (i.e. Quickbird imagery). Figure 2 shows a portion of this data that has been GIS-ready and comprises of city parcel records pronouncing the building footprints and building heights.

**RCS (Radar Cross Section) Simulation:** In this section, a basis for SAR index calibration is discussed. Considering the fact that SAR sensor is side-looking and since the cross-power term indicates a measure of the SAR image intensity and the fact that the radar return is highly dependent on the geometry of the imaging; such index must be calibrated for the entire scene. Urban environments can essentially be represented by a combination of different geometrical shapes (i.e. rectangular plates). The Envisat SAR system is consistent with a monostatic measurement/simulation that is the transmitter and the receiver are regarded as the same antenna and located at the same position with respect to the scene. It is expected that after a building collapses, the backscattering coefficient of the image is drastically reduced. The RCS values of the objects are highly sensitive functions of the sensor-object observation and object azimuth angles. The walls of the buildings and their adjacent pavements formed dihedral corner reflector. The RCS simulation is completed for VV polarization



Fig. 2: A portion of the 1:2000 urban digital map comprising of parcel data

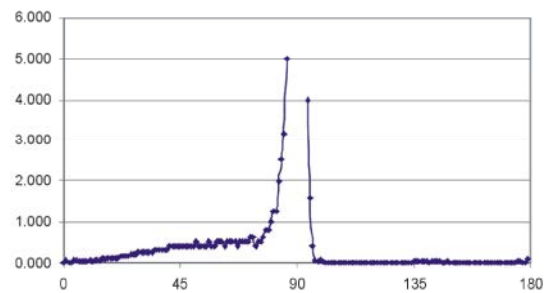


Fig. 3: VV polarization angle dependent RCS simulation curve for vertical dihedral reflector

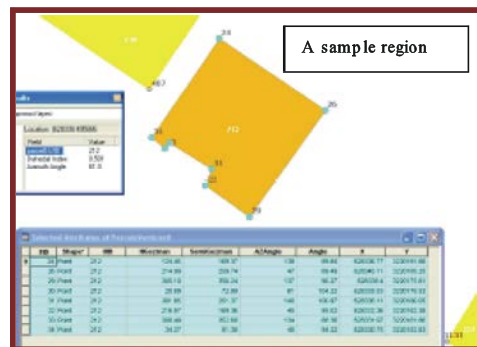


Fig. 4: Geo database analysis: detection of the most visible walls of the parcels (radar specific) [1]



Fig. 5: Parcel azimuth angle for the most visible walls (radar specific)

(specific to Envisat data) according to the vertical dihedral corner reflector and for one-degree increment in azimuth to cover the entire range. The effective area intercepting the beam is a function of the incident angle, the azimuth angle and also the intercepting area. Figure 3 is the simulated RCS value with respect to the azimuth angles.

**Implementation in GIS:** In order to apply the method for each parcel, the database (parcel records) was refined as to filter out all the buildings that are obscured. Moreover, analyzing each building footprint sides and corners; considering different angles, an automated process selects the most radar-detectable walls of the building. The corresponding azimuth angle is stored for each parcel record as shown in Figure 4. Then, the dedicated algorithm estimates the SAR signature based on the angle dependent RCS values for each parcel, then computes the calibration coefficients.

The azimuth angles are attributed for individual buildings (parcel record). Figure 5 shows the entire city of Bam; the very high resolution optical data as the base map and the color-coded parcels reflecting the azimuth angle of the most detectable walls in radar configuration. Angles around 82 degrees are close to the maximum radar reception in general since the satellite orbit is about 98 degrees near polar and the images are acquired in the descending pass.

## RESULTS AND DISCUSSION

Since the nature of the radar data is noisy and also coarse in term of resolution. A city block mask was also used for averaging out the change detection results. Therefore, two masks namely the parcel layer and the block layer were used in tandem. The parcel layer reflects the calibration coefficients and the building block layer reflects the averaged SAR change index values. The result of the rapid damage detection algorithm of this research is shown in Figure 6; where different levels of damage severity were made detectable.

The feasibility of change detection is evaluated according to an independent ground truth method that is counting the damaged buildings manually. Yamazaki *et al.* [7] have created a damage map (Figure 7) for Bam by visual interpretation of the VHR Quickbird optical data. They have used the EMS-98 damage grades and the process of assigning different building damage grades was fully manual. Table 2 summarizes their results in addition to the assumed equivalent damage factor ranges according to ATC13 report.

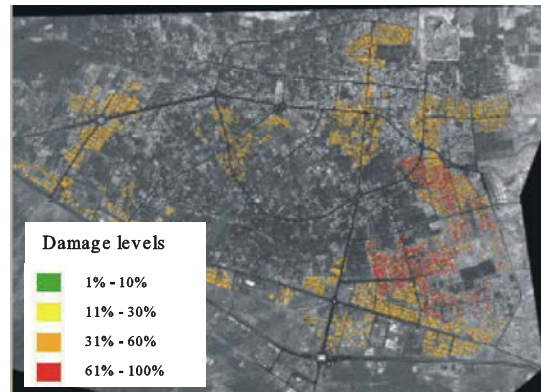


Fig. 6: Rapid SAR change detection results

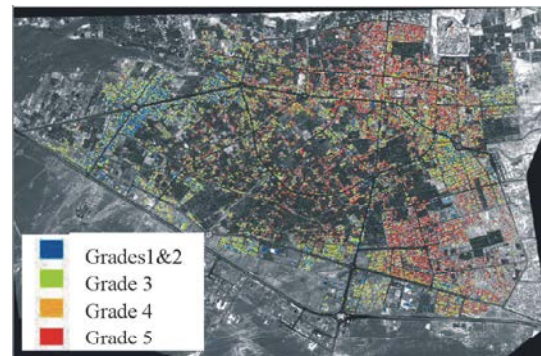


Fig. 7: SAR change detection by visual interpretation (courtesy of Yamazaki et al. [7])

Table 2: Visually interpreted damage grades and corresponding ATC13 damage factor

Damage grade assigned	No. of buildings interpreted	Assumed equivalent damage factor in ATC13	
		Range, %	Central, %
Grades 1& 2	1597	1-10	5
Grade 3	3815	10-30	20
Grade 4	1700	30-60	45
Grade 5	4951	60-100	80

Observing the rapid damage detection map of Figure 6 and comparing to the results illustrated in Figure 7, the major parts of hard hit zones were made feasible to detect with the expense of some existing false alarms. The coarse resolution of the SAR data that overlaps different features within each pixel and the presence of inherent noises within radar images in one hand and the complexity of the geometric configuration of urban settings with respect to radar detection on the other hand exhibit some limitation on the accuracy. However, for a rapid process of mapping hard hit zones right after large earthquakes in remote areas and for preliminary disaster management activities such as search and rescue, and resource allocation, the findings of such studies show

exceptional merits. It is emphasized that such modeling will be improved drastically by the use of very high resolution radar imageries.

#### **ACKNOWLEDGMENT**

This research was completed as part of a research contract between International Institute of Earthquake Engineering and Seismology with the municipality of Tehran (TDMMO) (contract # 190/503605). Professor Yamazaki is acknowledged for providing the authors with the visual damage interpretation data for the Bam earthquake.

#### **REFERENCES**

1. Mansouri, B., M. Shinozuka, C.K. Huyck and B. Houshmand, 2005. Earthquake-Induced Change Detection in Bam, Iran, by Complex Analysis Using Envisat ASAR Data. *Earthquake Spectra*, 1(21): 275.
2. Matsuoka, M. and F. Yamazaki, 2005. Building damage mapping of the 2003 Bam, Iran, earthquake using Envisat/ASAR intensity imagery. *Earthquake Spectra*, Special Issue. 1(21): 285.
3. Huyck, C.K., B.J. Adams, S. Cho, H. Chung and R.T. Eguchi, 2005. Towards rapid citywide damage mapping using neighborhood edge dissimilarities in very high-resolution optical satellite imagery – Application to the 2003 Bam, Iran earthquake. *Earthquake Spectra*, Special Issue. 1(21): 255.
4. Definiens Imaging, 2004. E-Cognition 4.0, User guide, Definiens Imaging GmbH, Munich, Germany.
5. Chen, Z. and T. Hutchinson, 2010. Probabilistic urban structural damage classification using bitemporal satellite images. *Earthquake Spectra*, 26(1): 87-109.
6. Mansouri, B. and M. Shinozuka, 2005. SAR image calibration by urban texture: Application to the BAM earthquake using Envisat satellite ASAR data. 3rd International Workshop on Remote Sensing for Post-Disaster Response, 12<sup>th</sup> and 13<sup>th</sup> September 2005, Chiba, Japan.
7. Yamazaki, F., Y. Yano and M. Matsuoka, 2005. Visual Damage Interpretation of Buildings in Bam City Using Quickbird Images Following the 2003 Bam, Iran, Earthquake. *Earthquake Spectra*, Special Issue 1(21): 329.